

# Analysis of Strain Nonuniformity Index (SNI) in electrohydraulically formed sheet metal component

S. K. Salunke<sup>1)</sup>, P. P. Date<sup>1)</sup>

<sup>1)</sup> Department of Mechanical Engineering, Indian Institute of Technology, Bombay, India

## Abstract

*In sheet metal parts formed by Electrohydraulic (free forming) process, a spherically shaped reflector is predicted to result in a highly non-uniform thickness strain distribution. As expected, the thickness strain (and hence thinning) is maximum at the top of the formed dome. The probability of failure is therefore highest at this location. A finite element model is formulated in ABAQUS explicit to generate the strain distribution in sheet metal. The model considers a water filled chamber to transmit the pressure pulse. The effect of the electrical discharge between the electrodes is modeled as a pressure wave of a certain magnitude originating from the location of the electrodes. The constitutive relation for the sheet is described by the Johnson-Cook model and non-deformable/ stiff tools are used.*

*The extent of non-uniformity in thickness strain distribution has been expressed in terms of Strain Non-uniformity Index (SNI). It is the difference between the peak thickness strain (PTS) and the average thickness strain (ATS). For successful forming, the value of SNI should be as low as possible. This is enabled by an alternate design of the reflector which is compared with the spherical shape. The pros and cons of using either shape of reflector are examined in the paper.*

## Keywords

Electrohydraulic forming, Thickness strain, SNI analysis

## 1 INTRODUCTION

The conventional approach to sheet metal forming uses two-sided tooling (e.g., solid die and a solid punch) and involves metal-to-metal contact between the punch, die and the work piece to achieve forming. This introduces certain difficulties, given increasing strength (requiring greater forming force and better lubrication to overcome the higher force of friction) and hardness of the metals that are being formed. Also, conventional sheet metal forming

processes use significant amounts of energy to form the sheet metal. Despite all efforts, the strain distribution remains highly non-uniform on account of frictional effects inhibiting sheet deformation at regions in contact with the tools, thereby shifting deformation to the 'unsupported region'. This makes it difficult to form thin, high strength sheet material used to produce very thin automotive panels required to significantly decrease the weight of the automobiles. [2, 5]

Electrohydraulic forming (EHF) is a high-rate forming process based on the high-voltage discharge of capacitors between two electrodes positioned in a fluid-filled chamber. Since pressure is transmitted through a liquid medium, the distribution of pressure is expected to be more uniform than when conventional tools are used. One therefore expects a better uniformity of strain distribution over the deformed sheet compared to the conventional forming route. EHF process is extremely fast; uses lower-cost, single-sided tooling; and allows significantly increased formability for many sheet metal materials because it involves high strain rates [1]. Setup time, which presently is relatively high, can be reduced by automation. Advancements in the EHF process have the potential to reduce the thickness variation of sheet metal used in the construction of automobile panels and frames. The application of EHF by automotive manufacturers and their suppliers will significantly enhance the product quality, compared to the conventional stamping process.

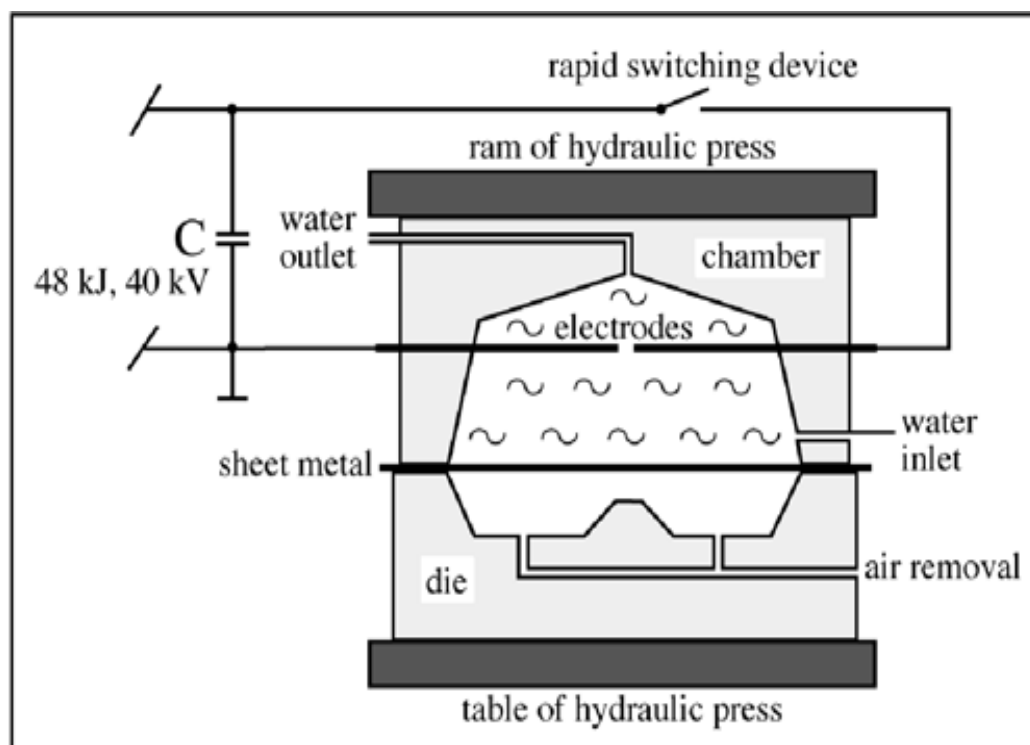


**Figure 1:** Basic Principle of Electrohydraulic forming [1]

Mathematical modeling of high-speed forming processes is widely used for various ends. In the present work, the effect of reflector geometry in electrohydraulic forming, on the resulting pressure and true thickness strain distribution is studied. A spherical reflector (representing a relatively simple geometry) is compared with that of the less simple geometry of a convex reflector with reference to pressure and thickness strain distributions.

## 2 FINITE ELEMENT SIMULATION

Electrohydraulic forming simulation is a considerable challenge because of the Multiphysics nature of the process. At first electrical energy must be converted into plasma. There is a boundary between the high pressure plasma and high pressure water vapor, and a boundary between the water vapor and the liquid. The liquid interfaces with the steel blank, and the steel blank accelerates and interacts with the die surface. Models must therefore be developed for: 1) the electrical nature of the discharge channel or plasma; 2) physical water vapor channel; 3) the liquid as a pressure transmitting medium; 4) blank deformation; 5) chamber (tool) deformation and 6) the blank in contact with the die [3].

Since, Electrohydraulic forming process is high strain rate process and completes within few microseconds, following simplifying assumptions are made here in simulations:

1. Heat transfer via heat conduction is neglected;
2. Phase conversion from water to vapor is neglected entirely;
3. All energy that is discharged into plasma is considered to contribute to the generation of blast waves only;
4. Plasma is treated as a gas with a constant mass that is surrounded by an acoustic medium (water), in which blast waves are generated;
5. Time lag between the direct and reflected incident waves is negligible owing to small size of the work piece investigated, and relatively high velocity of shock waves.

A dynamic explicit Finite Element analysis was carried out to simulate the Electrohydraulic Forming process. The program used for the simulation is ABAQUS Explicit. The water is the media which transmits the shock waves which in turn deform the blank. Water is shaped as the inside surface of the chamber that contains it. In the EHF experiment the pressure is build up by an electric discharge in the rear end of the water containing chamber, which in the simulation is represented by pressure wave generated at the point shown in Figure 2.

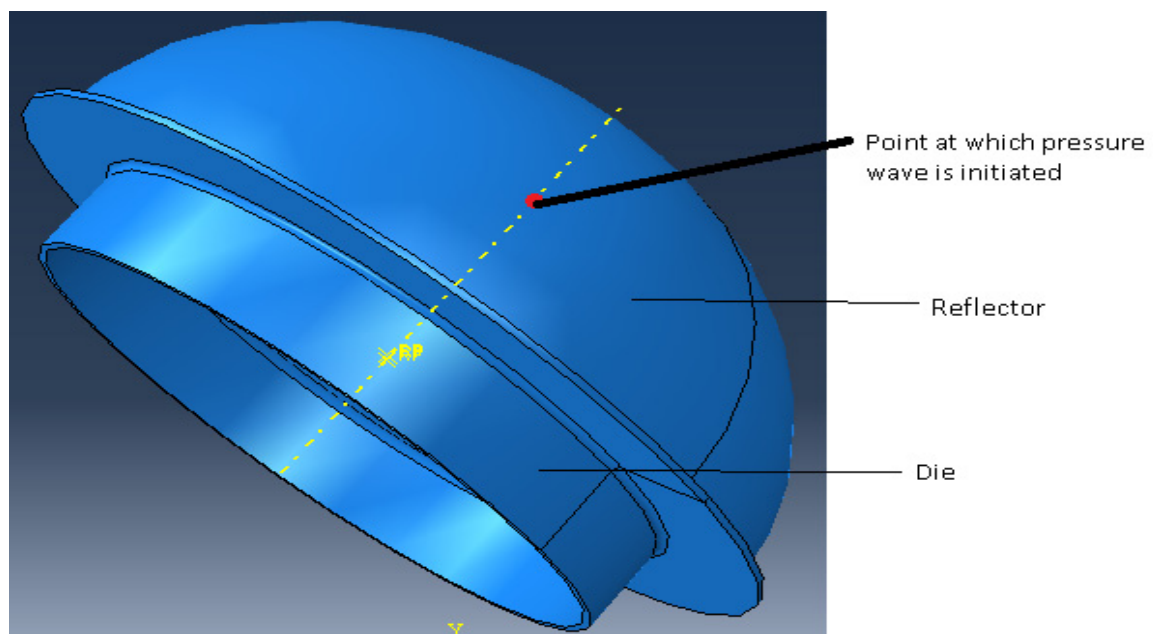


**Figure 2:** Assembled model used in simulation

## 2.1 Material Properties

### Blank:

The JC model is a widely used and well recognized model for high strain rate material deformation analysis, [4]

$$\sigma = [a + b(\varepsilon)^n] \left[ 1 + C \ln \left( \frac{\dot{\varepsilon}}{\dot{\varepsilon}_0} \right) \right] \quad (1)$$

**Table 1:** Material property for the simulated sheet material [2]

Steel grade	IF 210
Johnson Cook A, [MPa]	300
Johnson Cook B, [MPa]	344
Johnson Cook, C	0.03
Johnson Cook, n	0.53
Strain rate, (1/s)	0.01
Density $\rho$ , (kg/m <sup>3</sup> )	7800
Poisson's ratio, $\mu$	0.3
Young's Modulus, E [GPa]	210

### Water:

The property for the water was set to an acoustic medium with a density of 1000 [kg/m<sup>3</sup>] and a bulk modulus of  $2.3 \cdot 10^9$  [Pa].

- The bulk modulus

$$K = -V \left( \frac{\partial \rho}{\partial v} \right) \quad (2)$$

- The speed of sound,

$$c = \sqrt{\frac{K}{\rho}} \quad (3)$$

## 2.2 Interactions

The contact interaction between die and blank is set to a surface to surface condition, with contact property, tangential behavior and a friction coefficient of 0.1 in penalty contact. The incident wave interaction is used to specify magnitude of pressure at source point.

### 2.3 Load

The driving force in the EHF process is the electric discharge above the sheet. In the model it is represented by the pressure wave originating on the common axis of the chamber and the circular blank at distance of 50 mm from the top of the blank. The normalized pressure pulse variation with time is shown in Figure 3. It is seen that the pressure at the point of discharge (origin of the pressure pulse) dies down in about 100 microseconds.

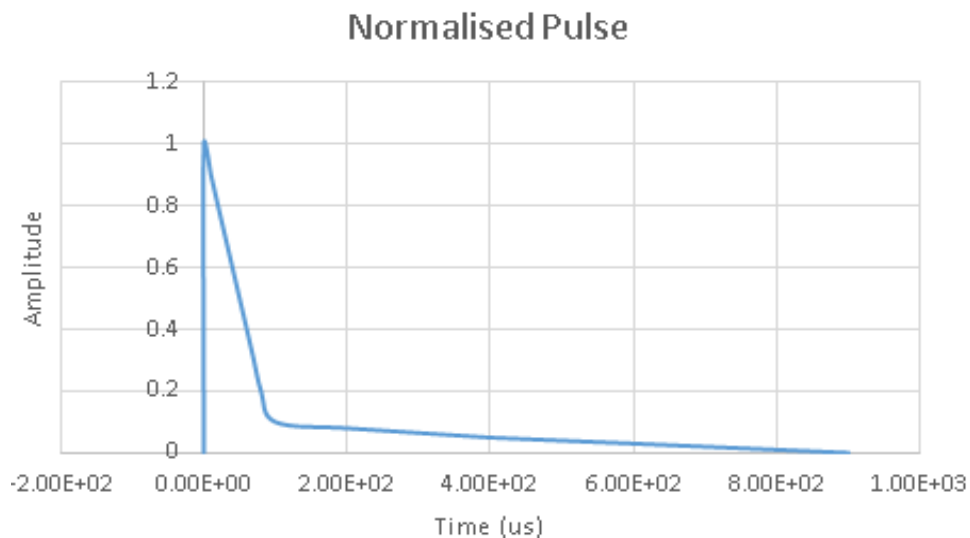


**Figure 3:** Normalized Pulse used for the simulation in ABAQUS

### 2.4 Reflector geometries

The geometries of the two reflectors used in the study are spherical and convex as shown in Figure 4. A spherically shaped reflector is predicted to result in a comparatively non-uniform thickness strain distribution than convex reflector.

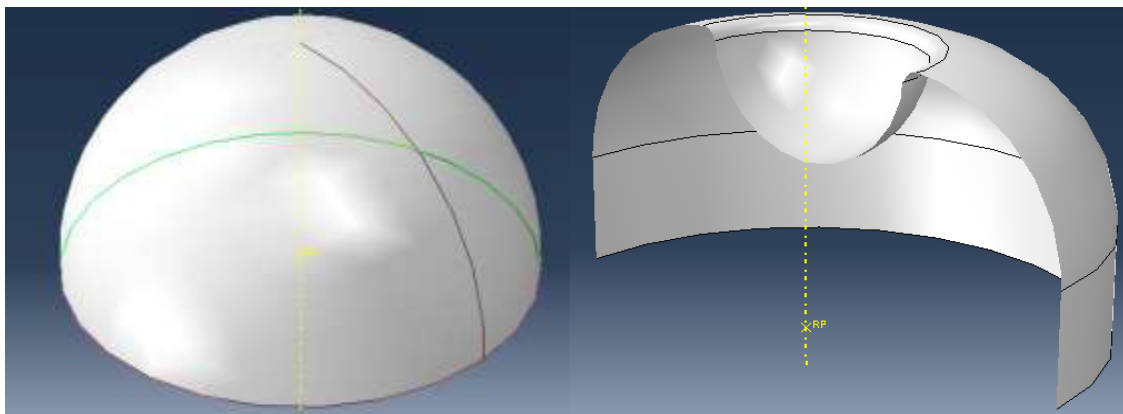


**Figure 4:** Two shapes of reflectors used in simulations-1) Spherical, 2) Convex

### 3 SIMULATION RESULTS

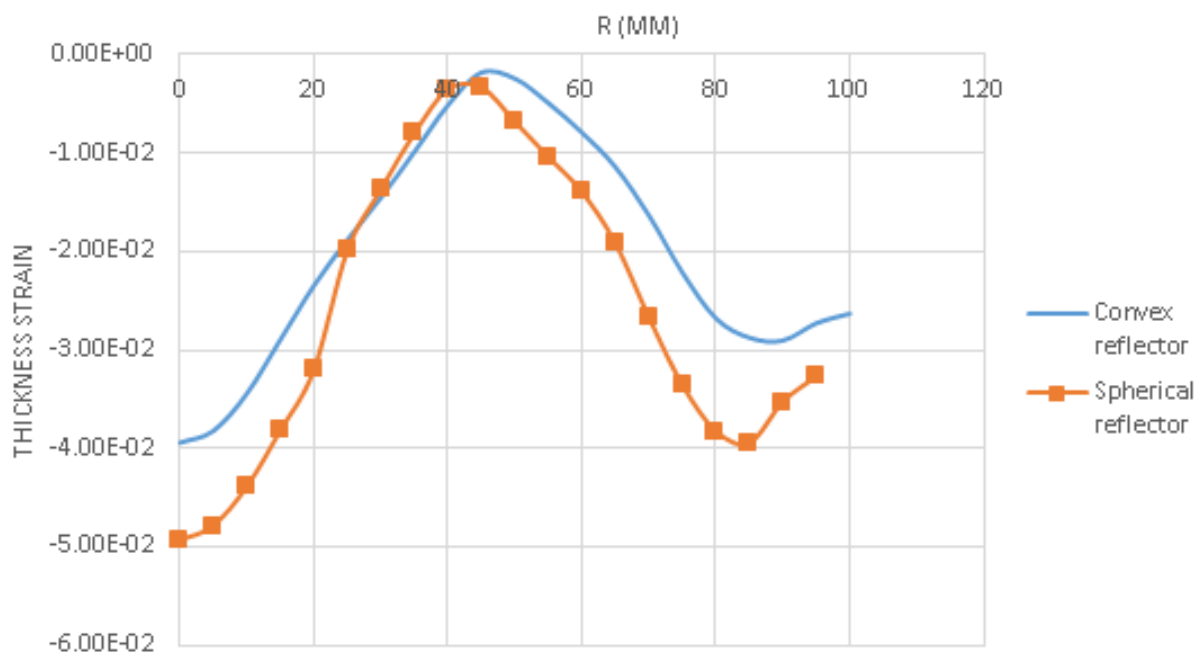
As expected, the thickness strain is maximum at the top of the formed dome. The probability of failure is therefore highest at this location. The extent of non-uniformity in thickness strain distribution has been expressed in terms of Strain Non-uniformity Index (SNI). It is the difference between the peak thickness strain (PTS) and the average thickness strain (ATS) [6].

$$SNI = PTS - ATS \quad (4)$$

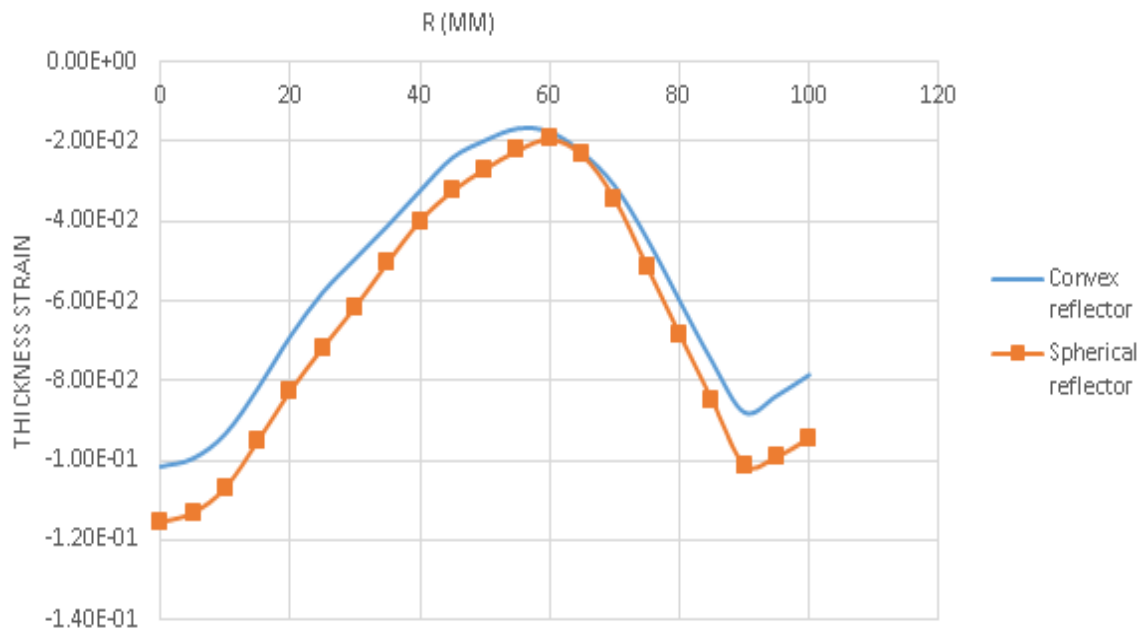
From figure 5 it is clear that spherical reflector results in high thickness strain at the top of dome.

#### 3.1 Strain distribution

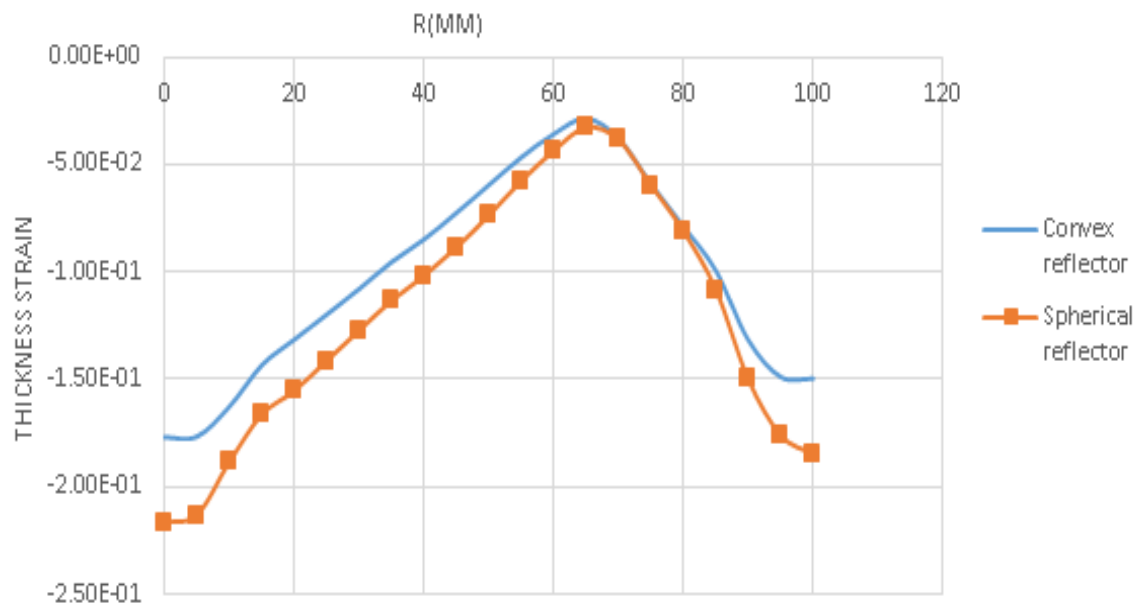
The true thickness strain variation along the radius is shown in figures 5, 6 and 7 for the two reflectors. It may be noted that the minimum true thickness strain occurs radially outward (at a greater radius) in a convex reflector at low depths as compared to the spherical reflector. The reverse is true at higher depths. With increasing depth of forming, this point of minimum thickness strain is seen to move away from the center for both the reflector geometries. Table 2 shows the relative non-uniformity of thickness strain distribution in the form of the SNI. At low deformation, the SNI values do not differ very much. However, as the depth increases the difference in SNI also increases (figure 8). In all cases, the SNI for the spherical reflector is always higher than that of the convex reflector, indicating superior quality with a convex reflector.



**Figure 5:** Thickness strain variation for two reflectors (depth = 25mm)



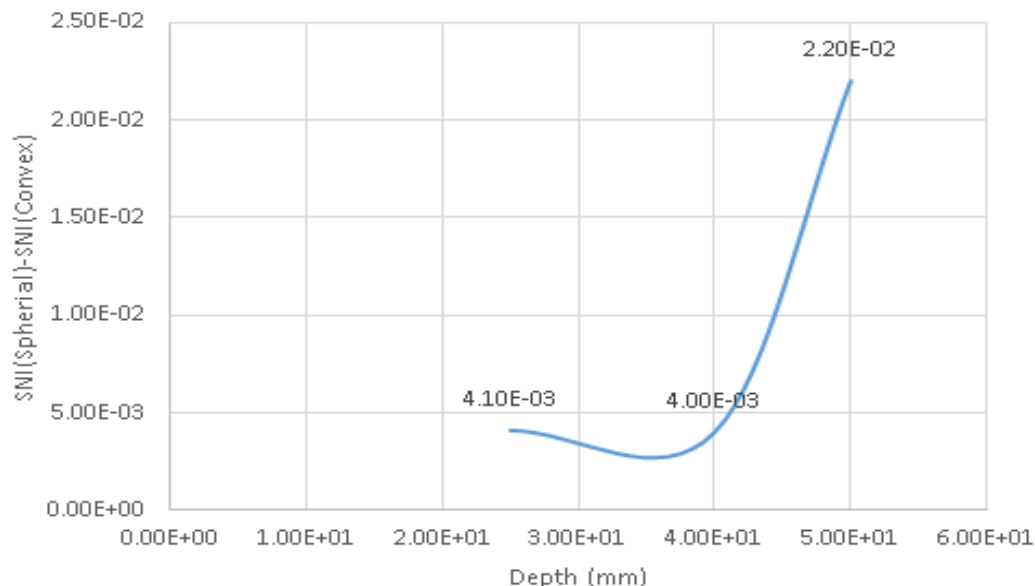
**Figure 6:** Thickness strain variation for two reflectors (depth = 40mm)



**Figure 7:** Thickness strain variation for two reflectors (depth = 50mm)

**Table 2:** SNI values for different depth of cup and reflector shapes

Depth of cup	Magnitude of pressure at source point (MPa)	Reflector type	Peak true thickness strain	Average true thickness strain	SNI
25mm	120MPa	Spherical	0.0494	0.0258	0.0236
		Convex	0.0394	0.0199	0.0195
40mm	240MPa	Spherical	0.1156	0.0664	0.0492
		Convex	0.1015	0.0565	0.045
50mm	300MPa	Spherical	0.2166	0.120	0.0966
		Convex	0.1766	0.102	0.0746

**Figure 8:** Difference in SNI values for spherical and convex reflectors for various depth of drawing

### 3.2 Pressure distribution

Pressure distribution at depths of 25mm and 50mm for the two reflectors is shown in Table 3. It may be inferred that the pressure distribution for both the reflectors for 25mm depth is very similar in trend and magnitude. The same is reflected in a minor difference between the SNI values for the two geometries. In contrast, the pressure distribution for the two reflectors between  $R = 0$  and  $R = 100$  is understandably different, though the shapes at a given time interval (100, 200 or 300 microseconds) are still somewhat similar. In particular, the pressure distribution is more similar at 100 microseconds and the similarity decreases with time. This also explains the increasing thickness strain variation (and hence the SNI) with increasing depth and time.



**Table 3:** Pressure distribution on the blank surface for two reflectors

Dept h	Spherical reflector	Convex reflector
25m m		
50m m		

#### 4 Conclusions:

From the foregoing, the following conclusions emerge:

1. The pressure distribution and hence the thickness strain distribution in a deforming sheet metal blank is sensitive to the shape of the reflector.
2. The convex reflector gives more uniform strain distribution (based on a lower value of SNI).

3. The trends observed in SNI variation with increasing depth (increasing forming energy) are well explained.
4. The similarity in pressure distribution at low depths and similar SNI are well understood. An increase in forming depth leads to an increase in difference between the SNI values and also dissimilarity between the two pressure distributions.
5. Further investigations are required into optimizing the shape of the reflector to obtain a uniform strain distribution even at large depths of deformation, i.e., a near zero value of SNI.

## References

- [1] *J. Varis, H. Martikka*: Prototyping of 3D sheet metal parts using electrohydraulic forming. ISSN 1392 - 1207, MECHANIKA, Nr.3 (53), p. 44-51, 2005.
- [2] *A. Melander, A. Delic, A. Bjorkblad, P. Juntunen, L. Samek, L. Vadillo*: Modelling of electro hydraulic free and die forming of sheet steels. International Journal of Material Forming, Vol. 6, p. 223-231, 2013.
- [3] *J. Bonnen, S. Golovashchenko, S. Dawson, A. Mamutov, A. Gillard*: Electrohydraulic Sheet Metal Forming of Aluminum Panels. Trends in Materials and Manufacturing Technologies TMS, p. 449-454, 2012.
- [4] *H. Huh, J. H. Lim and S. H. Park*: High speed tensile test of steel sheets for the stress-strain curve at the intermediate strain rate. International Journal of Automotive Technology, Vol. 10, No. 2, p. 195–204, 2009.
- [5] *W. Homberg, C. Beerwald, A. Pröbsting*: Investigation of the Electrohydraulic Forming Process with respect to the Design of Sharp Edged Contours. Proc. of the 4<sup>th</sup> International Conference on High Speed Forming, Columbus, Ohio, USA, 2010.
- [6] *S.G. Desai, P.P. Date*: On the quantification of strain distribution in drawn sheet metal products. Journal of Materials Processing Technology Vol. 177, p. 439–444, 2006.